Upgrading LHDGauss Code by Including Obliquely Propagating Wave Absorption Effect for ECH*)

Ryoma YANAI[1], Toru TSUJIMURA[1], Shin KUBO[1,2], Ryota YONEDA[3], Yasuo YOSHIMURA[1], Masaki NISHIURA[1], Hiroe IGAMI[1], Hiromi TAKAHASHI[1] and Takashi SHIMOZUMA[1]

[1]*National Institute for Fusion Science, National Institutes of Natural Sciences, 322-6 Oroshi-Cho, Toki, Gifu 509-5292, Japan*
[2]*Nagoya University, Furo-Cho, Chikusa-Ku, Nagoya 464-8601, Japan*
[3]*University of California Los Angeles, Los Angeles, CA, 90095, USA*

LHDGauss is a multi-ray tracing code to calculate microwave beam propagation and power deposition of electron cyclotron heating (ECH) using the electron density and electron temperature profiles in the Large Helical Device (LHD) plasma. LHDGauss also takes into account the injected wave polarization purity. LHDGauss uses the cold plasma dispersion to calculate ray propagation and derives the power absorption profile of ECH by using the absorption coefficient based on weakly relativistic plasmas and the wave propagating perpendicularly to the magnetic field. However, the ECH beam propagation is mainly oblique to the magnetic field in the LHD and it is necessary to take into account the angular dependence of the absorption coefficient in order to derive more accurate ECH power deposition profiles. We upgraded LHDGauss and were able to calculate the absorption coefficient using the weakly relativistic dielectric tensor which considers the influence of the angle between the magnetic field and the wave vector. We compared the power deposition profiles calculated by previous and upgraded LHDGauss with the changes of the electron temperature profile of the LHD plasma in the oblique and the perpendicular O1-mode ECH injection cases. We have obtained more reasonable power deposition profiles by using the upgraded LHDGauss in both the perpendicular and the oblique injection cases.

1. Introduction

ECH is one of the most essential auxiliary plasma heating methods using electromagnetic waves for magnetically confined fusion reactors. Its unique characteristic of local high power heating is important for not only plasma startup and heating but also for current drive and plasma profile control. Ray tracing and beam tracing methods are often used in order to calculate propagation and power absorption of microwave beams of ECH in plasma. 1 MW class gyrotrons of 77 GHz and 154 GHz are utilized in the LHD as the oscillation sources of ECH. The microwave beams from these gyrotrons are normally injected for the fundamental O-mode (O1-mode) or for the second harmonic X-mode (X2-mode) heating. Multi-ray tracing code "LHDGauss" has been developed at National Institute for Fusion Science and used for calculating the EC-wave beam propagation and the power deposition in the LHD because it can utilize the experimentally obtained electron temperature (T_e) and electron density (n_e) profiles and calculate the mode purity of the O-mode and the X-mode of microwave beams injected into the LHD plasma [1].

LHDGauss adopts the cold plasma dispersion for the calculation of ray propagation and uses the absorption coefficient based on the dispersion relation in weakly relativistic plasmas with the assumption that electromagnetic waves propagate perpendicularly to the magnetic field [2] for the calculation of power absorption. However, it is necessary to take into account the influence of the angle between the wavevector and the magnetic field on the absorption coefficient in order to obtain more accurate power deposition profiles because ECH is usually injected obliquely to the magnetic field in the LHD. Improving the power deposition calculation can help us to heat and control plasma more precisely and efficiently.

In this paper, we report the angular dependence of the absorption coefficient and the validity of the absorption coefficient by comparing the calculation with the experimental results regarding the O1-mode EC beam injection.

2. Upgrading of LHDGauss by Introducing New Absorption Coefficient

We refer to upgraded LHDGauss as LHDGauss-U in this paper. LHDGauss-U calculates multi-ray propaga-

*author's e-mail: yanai@nifs.ac.jp

tion by solving ray trace equations using the cold plasma dispersion relation, which is the same as the previous LHDGauss. On the other hand, LHDGauss-U calculates the absorption coefficient based on the dispersion relation in weakly relativistic plasmas derived by Volpe [3]. In Volpe's dispersion, the dielectric tensor ϵ_{ij} is expressed as

$$\epsilon_{ij} = \delta_{ij} + \frac{iX}{\beta_T^5 + \frac{15}{8}\beta_T^7} \sum_{n=-\infty}^{\infty} \sum_{m=|n|}^{\infty} \frac{(\lambda/2)^m Q_{mn,ij}}{\left(\frac{m+n}{2}\right)! \left(\frac{m-n}{2}\right)!}, \quad (1)$$

$$Q_{mn,ij} = \int_0^\infty \frac{dt}{\beta_T^2} \frac{Q_{ij}}{(1-it)^m}$$

$$\times \exp\left[\frac{it}{\beta_T^2}(1-nY) - \frac{\lambda + N_\parallel^2 t^2/2\beta_T^2}{1-it}\right], \quad (2)$$

$$\lambda = \left(\frac{N_\perp \beta_T}{Y}\right)^2, \quad (3)$$

$$\beta_T^2 = \frac{k_B T_e}{m_e c^2}, \quad (4)$$

$$X = \frac{\omega_{pe}^2}{\omega^2}, \quad (5)$$

$$Y = \frac{\omega_{ce}}{\omega}, \quad (6)$$

where ω is the frequency of the electromagnetic wave, ω_{pe} is the electron plasma frequency, ω_{ce} is the electron cyclotron frequency, c is the speed of light, k_B is the Boltzmann constant, m_e is the electron mass, $N_\parallel$ and $N_\perp$ are the refractive indices parallel and perpendicular to the magnetic field, respectively. Eq. (2) can be expressed as shown in Eqs. (35) - (45) of ref. [3]. Note that there seem to be some typographical errors regarding the summation convention in Eqs. (35) - (41). These equations include generalized Shkarofsky functions [4–6]

$$\mathcal{F}_{q,r}(z_n, a) = -i \int_0^\infty \frac{(it)^r}{(1-it)^q} \exp\left(iz_n t - \frac{at^2}{1-it}\right) dt, \quad (7)$$

$$z_n = \frac{1-nY}{\beta_T^2} - \lambda, \quad (8)$$

$$a = \frac{N_\parallel^2}{2\beta_T^2} - \lambda. \quad (9)$$

Note that z and a are shifted $-\lambda$ from the standard definitions. The absorption coefficient α is derived by

$$\alpha = 2 \frac{E_i^* \epsilon_{ij}^a E_j}{\left| E_i^* \frac{\partial \Lambda_{ij}^h}{\partial \mathbf{k}} E_j \right|}, \quad (10)$$

$$\Lambda_{ij} = \epsilon_{ij} + N_i N_j - N^2 \delta_{ij}, \quad (11)$$

where the superscripts ^{h} and ^{a} represent the Hermitian and anti-Hermitian part, E is the electric field and the superscript * represents the complex conjugate and $\mathbf{k}$ is the wavevector, respectively. We use E and $\mathbf{k}$ of the O-mode or the X-mode based on the cold plasma dispersion for calculating α. The equations (B.51), (B.53) and (B.54)

in ref. [7] are adopted to calculate generalized Shkarofsky functions except that a has a small or negative value, which means that the refractive index is mainly perpendicular to the magnetic field, because $\mathcal{F}_q(z_n, a)$ can not be defined in these equations. In this case, we adopt Dnestrovski functions,

$$F_q(z_n) = -i \int_0^\infty \frac{1}{(1-it)^q} \exp(iz_n t) dt, \quad (12)$$

which correspond to the limit of $\mathcal{F}_q(z_n, a)$ as a goes to zero [2, 3, 7]. Therefore, we can calculate both the obliquely propagating wave absorption ($N_\parallel > 0$) and the perpendicularly propagating wave absorption ($N_\parallel = 0$) and obtain the dependence of the absorption coefficient on the angle between the wavevector and the magnetic field since these equations include $N_\parallel$ and $N_\perp$.

Figure 1 indicates the angular dependence of the absorption coefficient of the O-mode wave calculated from the equations of perpendicularly and obliquely propagating waves derived by Bornatici [2], which are the simple approximate expressions, and the absorption coefficient calculated by Volpe's dispersion relation. Bornatici's absorption coefficients of obliquely propagating O-mode wave, which corresponds to the condition of $N_\parallel > \beta_T$, are given as Eq. (3.1.67) and Eq. (3.1.73) in ref. [2] for the fundamental and the high harmonic wave, respectively. The equation of the fundamental wave absorption coefficient is valid when the finite density plasma condition $(\omega_{pe}/\omega_{ce})^2 > 2\beta_T N_\parallel$ is satisfied. Additionally, Bornatici's absorption coefficients of perpendicularly propagating O-mode wave, which is equivalent to the condition of $N_\parallel < \beta_T$, are expressed as Eq. (3.1.40a) and Eq. (3.1.41)
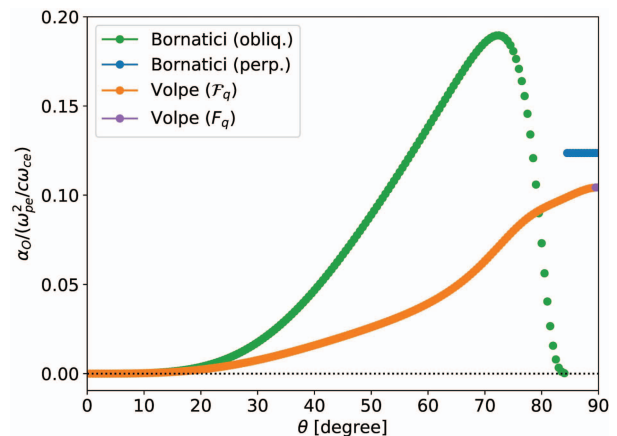

Fig. 1 Comparison of the angular dependence of the normalized absorption coefficient between Bornatici's equations [2] and Volpe's equations [3]. Calculating the absorption coefficient of Bornatici, (green) the oblique and (blue) the perpendicular propagation equations were switched at $N_\parallel = \beta_T$. Computing the absorption coefficient of Volpe, (orange) $\mathcal{F}_q$ and (purple) F_q were switched at $N_\parallel^2/2\beta_T^2 = 1.5\lambda$. The calculation parameters were $\omega_{ce}/\omega = 1.05$, $(\omega_{pe}/\omega_{ce})^2 = 0.55$, $T_e = 5$ keV and $\omega/2\pi = 77$ GHz.

in ref. [2] for the fundamental and the high harmonic wave, respectively. Those equations were adopted to calculate the absorption coefficient in Fig. 1. The absorption coefficients indicated in Fig. 1 were the sum of the harmonics up to the fifth in both Bornatici's case and Volpe's case although the fundamental component was dominant. The absorption coefficients of oblique propagation were mainly considered in the non-relativistic limit whereas the perpendicular propagation coefficients are derived for the weakly relativistic plasma in ref. [2].

Volpe's absorption coefficient continuously varies as the angle changes while Bornatici's absorption coefficient suddenly jumps when the equations switched those of perpendicular propagation to those of oblique propagation at $N_\parallel = \beta_T$. Although the Shkarofsky functions were switched to the Dnestrovski functions at $N_\parallel^2 / 2\beta_T^2 = 1.5\lambda$ to calculate the absorption coefficient, the dispersion relation (not shown) as well as the absorption coefficient were smoothly connected. LHDGauss uses only the perpendicular absorption coefficients expressed in Eq. (3.1.40a) and Eq. (3.1.41) in ref. [2]. Therefore, more reasonable results of the power deposition can be obtained by introducing the new absorption coefficient.

3. Experimental Setup

We analyzed the data of ECH power modulation experiments in order to investigate the validity of the new absorption coefficient regarding the O1-mode in the LHD plasma. The magnetic configuration was the magnetic axis $R_{ax} = 3.6$ m and the toroidal magnetic field $B_t = 2.85$ T. Figure 2 indicates the time evolution of the injected ECH power, central T_e and n_e in a typical discharge (#157201). The plasma was initiated by 77 GHz ECH#1 and sustained by two 154 GHz ECH of #4 and #5. The power of 77 GHz ECH#2 was modulated at 11 Hz during a steady-state period of the plasma. The injected power of each gyrotron was 0.7 - 0.8 MW. Figure 3 shows the radial profiles of T_e and n_e before injecting the power modulated ECH. T_e and n_e were approximately 3 keV and 1.5×10^{19} m^{-3} around the magnetic axis, respectively. The power modulated ECH#2 was injected obliquely (#157200) and perpendicularly (#157201) to the toroidal magnetic field as shown in the top panels of Fig. 4 to examine the difference of the T_e response. The EC beam was mainly injected as the O-mode and propagated to the magnetic axis from the launcher in both injection cases as indicated in the bottom panels of Fig. 4.

4. Comparison of ECH Power Deposition between Calculation and Experiment

The radial profiles of the power deposition and cumulative power of ECH#2 computed by LHDGauss-U and previous LHDGauss in the case of the oblique injection are
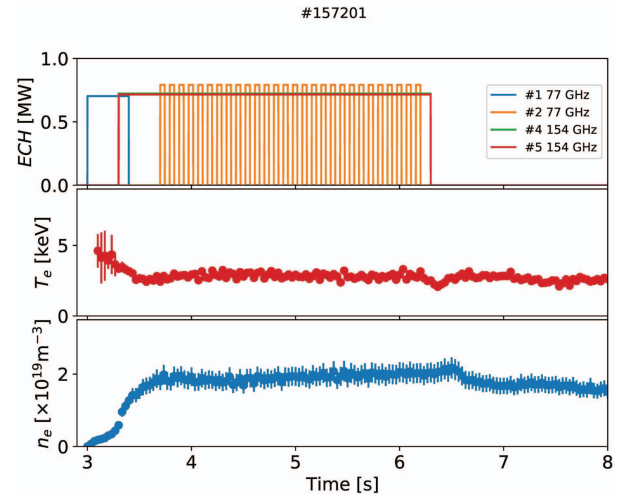

Fig. 2 Time evolution of (top) the injection power of ECH, (middle) T_e and (bottom) n_e around the magnetic axis in a typical plasma discharge. Blue and yellow lines indicate 77 GHz ECH power and green and red lines indicate 154 GHz ECH power in the top panel, respectively.
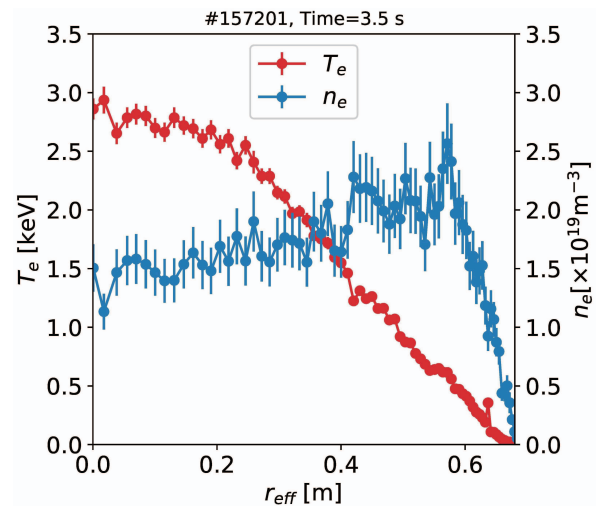

Fig. 3 Typical radial profiles of (red) T_e and (blue) n_e of the target plasma.

shown in Fig. 5. The absorbed power calculated by previous LHDGauss was concentrated in around $r_{eff} = 0.1$ m while the result derived by LHDGauss-U indicates that the power was absorbed in the broader region of $r_{eff} \leq 0.5$ m. On the other hand, similar power deposition profiles were obtained by LHDGauss-U and previous LHDGauss in the perpendicular injection and the power was mostly absorbed in the region of $r_{eff} \leq 0.2$ m (Fig. 6). In both cases, the ECH power was fully absorbed in the plasma as shown in the bottom panel of Fig. 5 and Fig. 6.

The change of T_e profiles by the ECH power modulation were analyzed by using the conditional average technique [8] of T_e measured by Thomson scattering measurement. The top panels of Fig. 7 and Fig. 8 show the radial
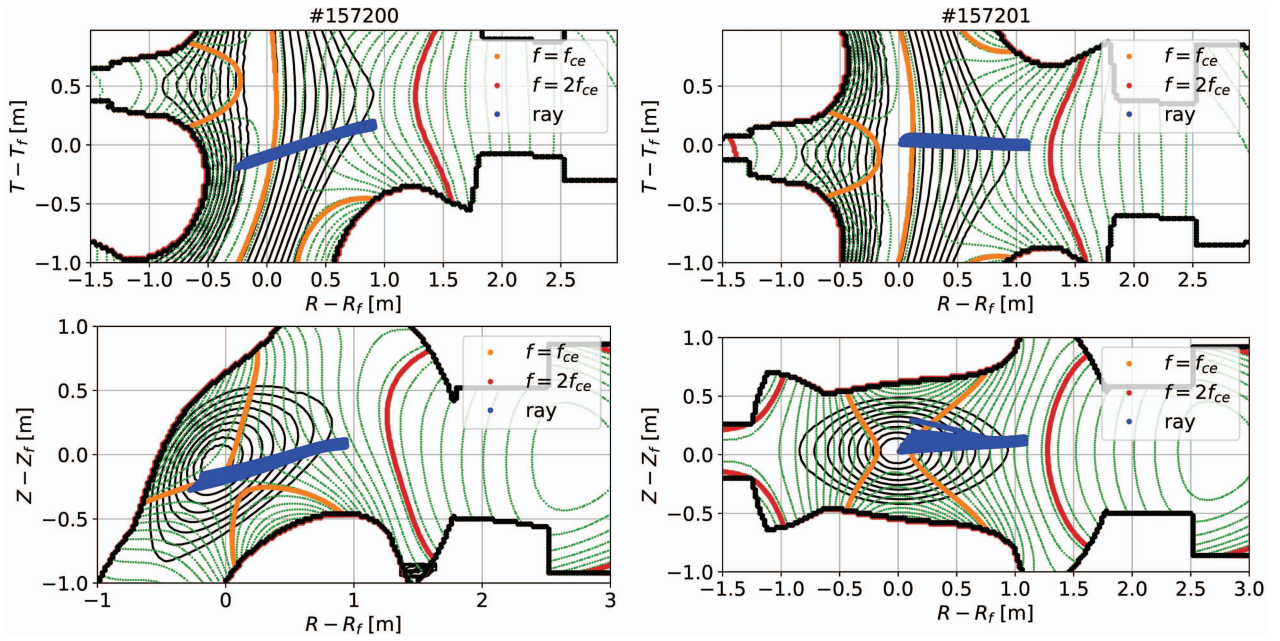
Fig. 4   Ray propagation of ECH#2 computed by LHDGauss-U (left top) on the cross-sectional plane containing the vector of the toroidal direction and the wavevector of injection waves and (left bottom) on the cross-sectional plane containing the vector of the vertical direction in the oblique injection case (#157200) and (right top and bottom) the same cross-sections except in the perpendicular injection case(#157201).
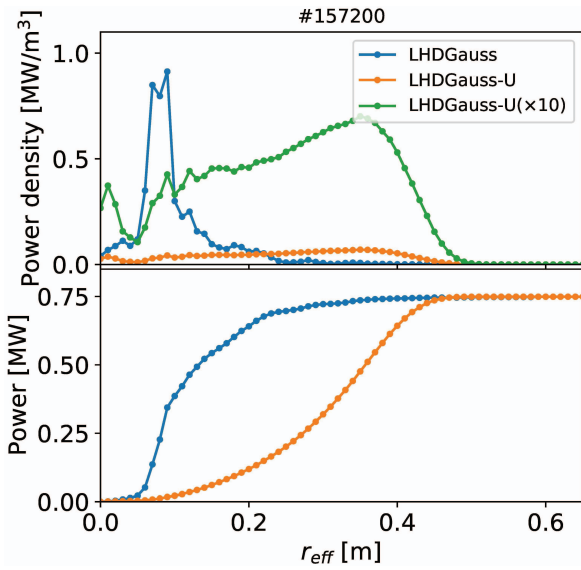

Fig. 5   Radial profiles of (top) the power deposition and (bottom) the cumulative power calculated by LHDGauss and LHDGauss-U for the oblique ECH injection. The green line in the top panel indicates the 10 times enlarged power deposition profile calculated by LHDGauss-U.

Fig. 6   Same as Fig. 5 except for the perpendicular ECH injection.

profiles of T_e averaged over the duration with ECH and without ECH. The bottom panels of Fig. 7 and Fig. 8 indicate the radial profiles of the electron temperature difference δT_e between the ECH-on and ECH-off duration. T_e increased in the off-axis region of $0.2\,\mathrm{m} \le r_{eff} \le 0.6\,\mathrm{m}$ and
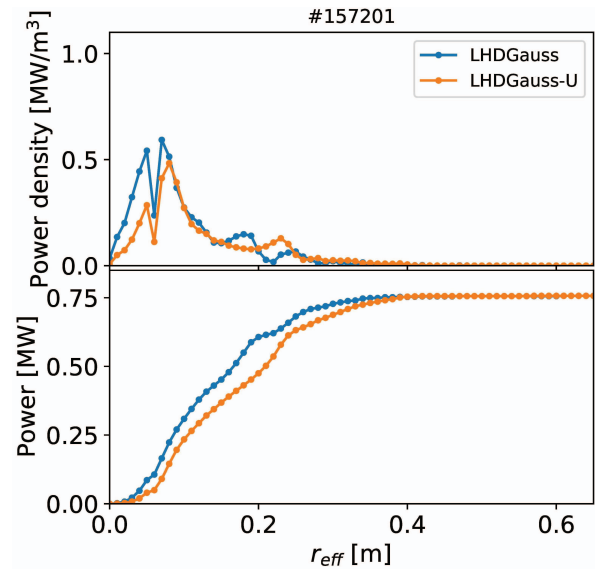
δT_e was maximized around $r_{eff} = 0.4$ m by the oblique ECH injection as shown in Fig. 7. By contrast, Fig. 8 indicates that T_e increased around the on-axis region and δT_e was the highest around $r_{eff} = 0.1$ m by the perpendicular ECH injection. These δT_e profiles had similar tendencies to the power absorption profiles obtained by LHDGauss-U in both of the oblique and the perpendicular injection.
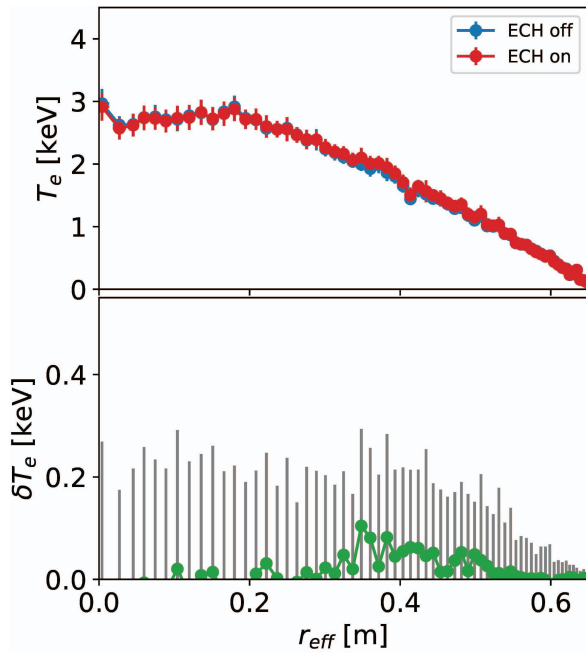
Fig. 7 (top) Radial T_e profiles of (blue) ECH-off and (red) ECH-on period and (bottom) the profile of the difference of T_e between ECH-on and ECH-off for the oblique ECH injection.
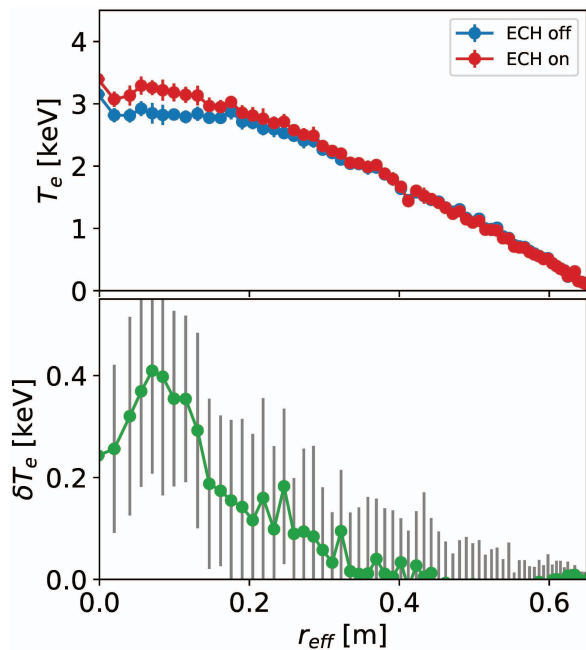

Fig. 8 Same as Fig. 7 except for the perpendicular ECH injection.

5. Conclusion

We introduced the new absorption coefficient into LHDGauss. This absorption coefficient takes into account the dependence of the angle between the wavevector and the magnetic field. The absorption coefficient smoothly changed with the angle. Comparing the ECH power deposition profiles of the O1-mode with the radial profile of the increase of T_e by ECH in the LHD plasma, the results calculated by LHDGauss-U resemble δT_e profiles in both of the perpendicular and the oblique ECH injection. On the other hand, the power deposition profile of previous LHDGauss had similar tendencies only with the δT_e profile of the perpendicular ECH injection. According to these results, we conclude that the more reasonable power absorption coefficient can be calculated and more accurate power deposition profiles can be obtained by using the new calculation method.

LHDGauss-U can provide more accurate results than the previous LHDGauss and it has been already utilized to analyze some experimental data [9, 10]. However, LHDGauss-U requires a significant amount of time to compute the absorption coefficient compared to LHDGauss because LHDGauss-U needs to calculate the dielectric tensor. Therefore, we will attempt to reduce the calculation time by optimizing the code as a next step, which will help us to use ECH more efficiently and safely.

[1] T. Ii Tsujimura *et al.*, Nucl. Fusion **55**, 123019 (2015).
[2] M. Bornatici *et al.*, Nucl. Fusion **23**, 1153 (1983).
[3] F. Volpe, Phys. Plasmas **14**, 122105 (2007).
[4] P.A. Robinson, J. Math. Phys. **27**, 1206 (1986).
[5] I.P. Shkarofsky, Phys. Fluids **9**, 561 (1966).
[6] V. Krivenski *et al.*, J. Plasma Phys. **30**, 125 (1983).
[7] D.G. Swanson, *Plasma Waves, 2nd edition* (Institute of Physics Publishing, Bristol, 2003) p.203-206, 407-409.
[8] T. Kobayashi *et al.*, Rev. Sci. Instrum. **87**, 043505 (2016).
[9] T. Kobayashi *et al.*, Plasma Fusion Res. **15**, 1402072 (2020).
[10] T. Ii Tsujimura *et al.*, Nucl. Fusion **62**, 026012 (2021).